Journal of Science and Technology – Engineering and Technology for Sustainable Development
Volume 36, Issue 3, July 2026, 061–069

Effect of Electrolyte Additives for Suppressing Zinc Dendrites in Rechargeable Zinc-Ion Batteries: Preliminary Study

Nguyen Thi Tra My[1], Bui Thu Uyen[1], Le Thi Thu Hang[1,2,*]
[1]School of Chemistry and Life Sciences, Hanoi University of Science and Technology, Ha Noi, Vietnam
[2]Institute of Energy Technology, Hanoi University of Science and Technology, Ha Noi, Vietnam
[*]Corresponding author email: hang.lethithu@hust.edu.vn

Abstract

Aqueous zinc-ion batteries (AZIBs) offer safety, low cost, and material abundance. However, their performance is limited by dendrite formation, side reactions, and poor cycling stability. The study preliminarily examines the effects of various additives in aqueous electrolytes on the electrochemical behaviour of AZIBs by using contact angle, pH value, Hull cell, cyclic voltammetry (CV), electrochemical impedance spectroscopy (EIS), and linear scan voltammetry (LSV) measurements. The additives under investigation include urea, thiourea, serine, tyrosine and tryptophan, which are known as low toxicity and biodegradable compounds. The obtained measurement results indicate that inclusion of the additives into the blank electrolyte of 1 M $ZnSO_4$ at the low concentration of 5 mM only induced slight change in the pH of the electrolyte, which had no significant impact on the corrosion behaviour of a zinc metal anode in the electrolyte. In addition, the contact angle of zinc metal with the electrolytes remained at values smaller than 90°, demonstrating the hydrophilicity of the zinc anode after addition of the additives. Among the investigated organic additives, urea, thiourea, and tyrosine demonstrated mitigation of zinc dendritic growth as well as inhibition of parasitic reaction (hydrogen evolution reaction). However, at high concentrations (10–100 mM) the additives promoted the dendritic growth. The further intensive investigations are recommended to deploy, thus highlighting the role of targeted additive selection in enhancing the durability and operational safety of aqueous zinc-ion batteries.

Keywords: Additives, aqueous zinc-ion batteries, anticorrosion, dendrite suppression, hydrogen evolution.

1. Introduction

In modern society, with an increasing demand for energy, continued combustion of non-renewable traditional energy resources not only depletes the available resources, but also worsens global warming. Therefore, the exploration and utilization of renewable sources for energy production is necessary. Renewable green energy sources include solar, wind, hydropower, geothermal, and biomass energy. All these energy resources are renewable, abundant, sustainable, cost-effective, and clean (little or no carbon emissions). However, the supply of renewable energy fluctuates with time and the season in years. To effectively use renewable energy sources, development of a novel energy storage and conversion system is indispensable. Currently, rechargeable lithium-ion batteries have been used increasingly in portable electronic devices and hybrid transport vehicles because of their own advantages such as light weight, fast response, a low self-discharge rate, and less maintenance [1]. However, LIBs show cost-, and safety-related problems. Specifically, the use of organic electrolytes is one of the causes of the risk of explosions and fire in LIBs. Thus, this has triggered research interest world-wide to develop new battery technologies having safe, stable and high performance.

Among various candidates, aqueous zinc-ion batteries (AZIBs) have emerged and attracted increasing attention due to their high theoretical capacity (820 $mAh \cdot g^{-1}$, 5855 $mAh \cdot cm^{-3}$), low redox potential (−0.76 V vs. SHE), abundant and low-cost raw materials, intrinsic safety, and the high ionic conductivity of aqueous electrolytes [2-4]. Unlike LIBs or sodium-ion batteries employing flammable organic electrolytes, AZIBs use water-based electrolytes, which minimize fire hazards and reduce environmental toxicity [5]. Although AZIBs possess plenty of advantages, their practical deployment is still hindered by several critical issues associated with the zinc anode. The issues include uncontrolled dendritic growth, and side reactions such as hydrogen evolution reaction (HER), corrosion, and surface passivation during repeated Zn plating/stripping cycles [6-8]. These phenomena not only degrade Coulombic efficiency and cycling stability but can also cause short-circuits and mechanical failure of a separator in AZIBs.

Regarding uncontrolled dendritic growth, according to the previous reports, dendrite formation is mainly driven by inhomogeneous current distribution, localized electric field intensification (tip effect), and the solvation structure of Zn^{2+} in aqueous electrolytes [9-10].

p-ISSN 3093-3242
e-ISSN 3093-3579
https://doi.org/10.51316/jst.191.etsd.2026.36.3.9
Received: Oct 29, 2025; Revised: Dec 9, 2025
Accepted: Dec 26, 2025; Online: Feb 20, 2026.

Furthermore, the high activity of water molecules facilitates HER and the formation of insulating by-products such as $Zn(OH)_2$ and $Zn_4SO_4(OH)_6{\cdot}xH_2O$, which block ionic transport and accelerate anode degradation [11, 12]. To date, various strategies have been developed to address these challenges, including artificial solid electrolyte interphase (SEI) layers [13], three-dimensional structured zinc hosts [14], alloying approaches [15], and electrolyte engineering [16]. Among mentioned strategies, electrolyte engineering is considered one of the most straightforward and scalable methods to enhance the performance of metallic zinc anodes [17]. In addition to optimizing the salt type and concentration of the electrolyte for AZIBs, the introduction of electrolyte additives has proven particularly effectively. Additives inclusion in the electrolyte shows many benefits to AZIBs, for example, (i) modifying the Zn^{2+} solvation shell and hydrogen-bond network of water, (ii) promoting the formation of protective SEI-like interphases, (iii) homogenizing ion flux and guiding Zn deposition along preferred crystallographic planes, (iv) suppressing HER and corrosion, or (v) improving thermal and chemical stability of the electrolyte [18, 19].

A wide range of additives, including organic molecules, inorganic salts, polymers, and biomolecules, have been investigated [17]. In recent years, bio-derived additives such as amino acids (e.g., glycine, arginine, lysine) and polysaccharides (e.g., chitosan) have garnered attention owing to their environmental friendliness, low cost, and multifunctional regulation mechanisms [20-22]. These molecules can adsorb selectively onto the surface of Zn anodes, regulate the electric double layer, alter Zn^{2+} nucleation behavior, and stabilize the electrolyte–electrode interface, thereby extending cycle life and improving Coulombic efficiency. This demonstrates that the development of efficient, low-cost, and safe bio-derived electrolyte additives is a new research direction to overcome the existing limitations of AZIBs and advance their practical applications in large-scale energy storage.

In the present work, we report a preliminary study on the effects of some biomolecules including serine, tyrosine, and tryptophan as well as urea and thiourea as electrolyte additives for AZIBs. The aim of this research is to develop non-toxic and highly biodegradable electrolytes that enhance the electrochemical performance of AZIBs throughout addressing the issues related to Zn anodes. This approach opens opportunities for the development and commercialization of AZIBs in applications that demand superior safety and stability to LIBs.

2. Methodology

All chemicals including zinc sulfate ($ZnSO_4{\cdot}7H_2O$, 99.5%), serine ($C_3H_7NO_3$, 99%), tyrosine ($C_9H_{11}NO_3$, 99%), and tryptophan ($C_{11}H_{12}N_2O_2$, 99%), urea ($(NH_2)_2CO$, 99%) and thiourea ($(NH_2)_2CS$, 99%) were purchased from Xilong Scientific Co., Ltd. (China) and used without further purification. The electrolytes used in this study consisted of 1M $ZnSO_4$ (Xilong, China; purity 99%) with x mM organic additives of thiourea, serine, tyrosine, and tryptophan (x = 5, 10, 20, 50, and 100) by dissolving the purity chemicals with distilled water.

To evaluate electrochemical behaviour of the electrolytes, asymmetric Cu//Zn cells were assembled into CR 2032-coin cells. Wherein, a disc of Zn metal worked as counter and reference electrodes and a disc of Cu metal worked as a working electrode. The electrodes of a diameter of 16 mm were punched from copper foil (99.95%) and zinc foil (99.99%). A piece of Whatman glass fiber separator was cut into 16mm-disc-pieces. Prior to assembling a cell, the separator was soaked in 100 µL of the electrolyte.

Cyclic voltammetry (CV), electrochemical impedance spectroscopy (EIS), and linear scan voltammetry (LSV) measurements were conducted using a multi-channel workstation (AUTOLAB/PGSTAT302N) equipped with an FRA2 module (ECO CHEMIE, AUTOLAB, The Netherlands) and controlled via Nova 2.1 software. The electrochemical performance of asymmetric cells with different electrolytes was evaluated using CV at a scan rate of 5 mV s^{-1} within a potential window of −0.2 to 0.4 V. For EIS and LSV measurements, a three-electrode configuration cell was used. Wherein, a zinc metal electrode worked as a working electrode, a platinum mesh electrode served as a counter electrode and a saturated calomel electrode worked as a reference electrode. EIS measurements were performed at an open-circuit potential (OCP) in a frequency range of 0.1 Hz to 100 kHz with a perturbation voltage of 5 mV. The LSV measurements were carried out within the potential window of $\pm$ 300 mV vs. OCP. The inhibition efficiency (H_i) of the additives was calculated according to LP extrapolation analysis as follows [23]:

$$H_i = \frac{i_c^0 - i_c}{i_c^0} \times 100\% \quad (1)$$

where i_c^0 and i_c are corrosion current density in the electrolyte without and with the additive, respectively.

Besides, a Hull cell with a solution volume of 267 ml was utilized to evaluate the effect of the additives present in the electrolyte on the quality of electrodeposited zinc layers, as well as to allow to optimize a current density range for the plating Zn process. A cathode and an anode used in the Hull cell were copper panel and zinc panel, respectively. The current distribution was calculated based on the formula [24]:

$$i = I\,(5.1 - 5.24\,log_{10}X) \quad (2)$$

where i is current density ($A{\cdot}dm^{-2}$) and I is total current (A) and X is distance from high current density end of cathodic panel.

In addition, to record the growth process of Zn dendrites during the charge process of AZIBs a transparent symmetric cell of Zn/electrolyte/Zn was prepared, where the distance between two Zn electrodes was fixed to be 1 cm. Finally, the wettability and pH of the electrolyte with the presence of the additives were evaluated using a contact angle analyzer (DSA25, KRÜSS) and a portable pH meter (HANA). The measurements of water contact angles were performed at ambient temperatures with a volume of the test electrolyte droplets approximately 2 µL. Three different positions on the Zn surface were measured to obtain average contact angle values. Similarly, the pH measurements of the electrolytes with and without the additives were performed three times. The corresponding values reported in the present work are average values.

3. Results and Discussion

3.1. Effect of the Additive Composition

The pH of electrolyte is one of important specification parameters that determine the long-term cycle life of AZIBs. The anode of AZIBs is normally Zn metal, which has a negative reduction potential (−0.76 V vs. SHE), aggressive activity, and high corrosion rate in aqueous electrolytes, specifically, in acidic (pH < 6) and alkaline (pH >12.5) environments [25]. Thus, to interpret the effect of the additives on the stability of zinc anode in AZIBs, pH of the electrolytes with and without the additives under investigation was measured.

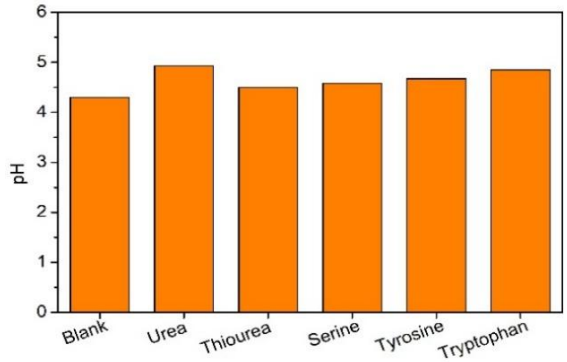

Fig. 1. pH of the electrolyte containing 1M $ZnSO_4$ in the presence of 5mM different additives

As shown in Fig. 1, in the absence of the additives, the electrolyte only containing 1 M $ZnSO_4$ (namely blank electrolyte) possesses an acidic environment with the pH value of 4.3. This suggests the existence of the self-discharge phenomenon of AZIBs, which possibly occurs due to the corrosion of the metallic zinc anode immersed in the acidic electrolyte. After inclusion of the 5 mM additives into the electrolyte, a slight increase in the pH of the electrolytes was recorded. In particular, the electrolyte with the presence of urea additive had the highest pH of 4.93, which is followed by the electrolyte containing tryptophan (pH of 4.85) and tyrosine (pH of 4.67). This can be explained by that, amino acids have both an amine group ($-NH_2$) and a carboxyl group ($-COOH$). The amine group can accept protons (H^+) in solutions, leading to a slight increase in pH, whereas the carboxyl group can react with the local H^+ to maintain the stabilized surface pH microenvironment. When OH^- is present in excess, the following reaction occurs:

$$RCH(NH_2)COOH + OH^- \rightleftharpoons RCH(NH_2)COO^- + H_2O \quad (3)$$

In contrast, when H^+ is excessive, the following reaction occurs as:

$$RCH(NH_2)COOH + H^+ \leftrightarrow RCH(NH_3)^+COOH \quad (4)$$

These results demonstrate that amino acids, as amphoteric additives, can adapt to pH changes and maintain a stable microenvironment by interacting with both H^+ and OH^- ions in the aqueous electrolyte. Meanwhile, urea is an amide. The molecule of urea only has two amine groups, but no carboxyl group. Thus, when urea is soluble in the aqueous electrolyte, more protons are accepted into the amine groups of urea. Accordingly, the electrolyte containing urea had the highest pH value. Regarding thiourea, among the additives, the electrolyte of the thiourea additive possessed the second lowest pH value (pH of 4.5), just after the blank electrolyte. Thiourea has a similar structure to urea with the oxygen atom replaced by sulfur but has less effect on pH due to its lower hydrogen-bonding ability, as well as molecular polarity. Hence, the measured pH results of the electrolytes allow us to infer that, among the tested additives, urea offers the highest efficiency in reducing self-discharge phenomenon for AZIBs owing to enhancing the pH of the electrolyte.

In addition to the pH environment, the electrolyte wettability at electrode substrate/electrolyte interfaces is also critical factor that governs electrochemical mechanism of AZIBs. So, in the present work, wettability behavior of the electrolytes containing the additives was investigated through contact angle measurements. Fig. 2 displays the change in the contact angle of metallic zinc substrate with the various electrolytes containing 5 mM additives of urea, thiourea, serine, tyrosine, and tryptophan.

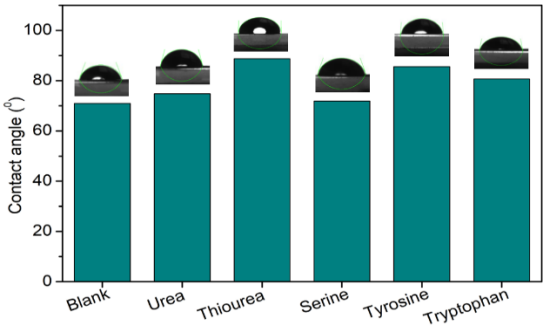

Fig. 2. Contact angle of the electrolyte containing 1M $ZnSO_4$ in the presence of 5 mM different additives

As observed in Fig. 2, as for the blank electrolyte, the measured contact angle was 70.98°. After inclusion of the additives in the electrolyte, the contact angle increased. In particular, the zinc substrate showed the contact angles of 74.77°, 71.9°, and 80.68° when measured for the electrolyte containing urea, serine and tryptophan, respectively. Remarkably, the measured contact angle exceeded 85° as for the electrolyte containing thiourea (88.79°) and tyrosine (85.59°). This indicates the increasing hydrophobicity of the surface of the zinc anode in the electrolyte in the presence of the additive. However, in general the measured contact angles of the electrolyte with and without additives were smaller than 90°, demonstrating the hydrophilicity of the zinc anode. According to the previous reports [4, 26-28], the inclusion of the additives promotes the preferential bonding between Zn^{2+} and additive molecules, as well as reduces the water content in the solvation structure of Zn^{2+} ions in the electrolyte, thereby inducing Zn uniform plating, suppressing dendrite growth, and mitigating water-related side reactions. Accordingly, the wettability of the electrolyte after adding additives will be improved, which is normally evidenced by the decrease in the contact angle of the additive-added electrolyte toward the zinc anode. Unfortunately, the electrolyte with the tested additives in the present work possessed a high contact angle compared to the electrolyte without additives.

Thus, to clarify the effect of these additives on the electrochemical performance of the metallic zinc anode, the cyclic voltammograms of the zinc plating/stripping processes were recorded within a potential range of −0.2÷0.4 V vs. Zn^{2+}/Zn at a scan rate of 5 $mV{\cdot}s^{-1}$. As shown in Fig. 3a, the shape of the obtained CV plot before and after adding the additives into the electrolyte almost remains. No strange reduction or oxidation peak was found, suggesting no occurrence of the redox reaction of additives within the investigated potential range. On the positive scan, only an anodic peak is observed at the potential from 0.14 to 0.22 V vs. Zn^{2+}/Zn, depending on the additives introduced into the electrolyte. This anodic peak corresponds to dissolution of Zn metal onto the foreign substrate (Cu substrate in the asymmetric Zn//Cu cell). The largest anodic peak (3.4 $mA{\cdot}cm^{-2}$) belonged to the thiourea-added electrolyte, followed by the tryptophan-added electrolyte (3.0 $mA{\cdot}cm^{-2}$), the serine-added electrolyte (2.8 $mA{\cdot}cm^{-2}$), and the urea-added electrolyte (2.7 $mA{\cdot}cm^{-2}$). At that time, the current density of the anodic peak of the blank electrolyte was 2.6 $mA{\cdot}cm^{-2}$, slightly higher than that of the tyrosine-containing electrolyte (2.3 $mA{\cdot}cm^{-2}$).

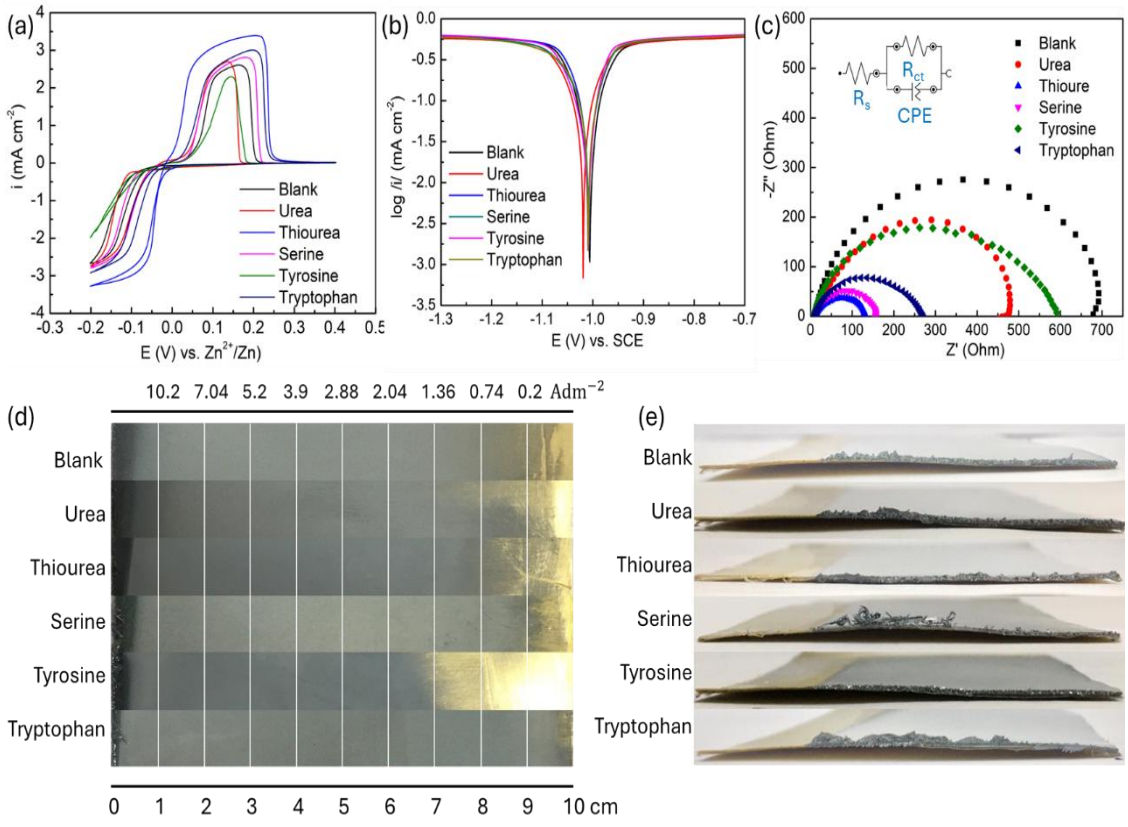

Fig. 3. (a) CV plots of Zn nucleation in Zn//Cu half-cells with various electrolytes containing 5 mM additives, (b) EIS plots, (c) Tafel plots, (d) surface images and (e) cross-section images of the zinc anode after electrodeposition at 2 A for 5 min, corresponding to a volumetric current density of 7.49 $A{\cdot}dm^{-3}$

Table 1. CV and LSV analysis data of Zn metal in the 1M $ZnSO_4$ electrolyte with and without 5 mM additives

Electrolyte	Q_{anodic} (A.s)	$Q_{cathodic}$ (A.s)	*CE* (%)	$E_{cor.}$ (V)	$i_{cor.}$ (mA·cm^{-2})	H_i (%)
Blank	16.52	11.95	72.34	-1.018	4.57	-
Urea	38.78	29.98	77.31	-1.028	4.34	5.03%
Thiourea	45.14	32.72	72.49	-1.013	4.17	8.75%
Serine	25.15	18.85	74.95	-1.013	2.85	37.64%
Tyrosine	26.98	21.34	79.11	-1.007	2.92	36.10%
Tryptophan	22.66	10.98	48.45	-1.015	1.75	67.70%

On the negative scan, although no cathodic peak corresponding to the deposition of Zn onto the Cu substrate as well as no cathodic peak corresponding to hydrogen evolution was recorded, a similar change in the maximum cathodic current density at −0.2 V vs. Zn^{2+}/Zn was recognized for the electrolyte with different additives. The results demonstrated that the additives had a significant impact on the kinetics of both zinc reduction/oxidation and hydrogen evolution reactions. From Fig. 3a, the calculated ratio of the charges for zinc dissolution and deposition, $Q_{anodic}/Q_{cathodic}$, which is well-known as Coulombic efficiency (denoted as *CE*), was 72.34%, 77.31%, 72.49%, 74.95%, and 48.45% for the electrolyte without and with urea, thiourea, serine, tryptophan, respectively (Table 1). Herein, the cathodic process includes zinc electrodeposition and hydrogen evolution reactions. Noticeably, as for the tyrosine containing-electrolyte, despite no promotion of the kinetics of both zinc reduction and hydrogen evolution reaction, the charge ratio held at a value of 79.11%, even higher than that of all the rest of the electrolytes. This demonstrates that introducing tyrosine into the electrolyte preferentially hindered hydrogen evolution rather than zinc reduction reaction. In contrast, among the electrolytes, the electrolyte with tryptophan possessed the lowest ratio of the charges for zinc dissolution and deposition (48.45%) despite enhancement in both anodic and cathodic current densities compared with the blank electrolyte. This means that tryptophan promoted both zinc deposition and hydrogen evolution reactions but preferentially promoted the latter.

On the other hand, as for the blank electrolyte, the onset potential of zinc nucleation was rather large (−94 mV vs. Zn^{2+}/Zn). Meanwhile, apart from urea, the electrolytes with serine, tryptophan, and thiourea show a shift in the onset potential of zinc nucleation toward less negative potential direction. In specific, the onset potential values of zinc nucleation of −88 mV, −48 mV, and −28 mV vs. Zn^{2+}/Zn were recorded for the electrolyte with adding serine, tryptophan, and thiourea, respectively. This demonstrates that the additives facilitated the zinc nucleation process, which possibly resulted in the rough and uneven zinc crystals deposition. Compared with the blank electrolyte, the electrolyte after inclusion of urea had a nucleation overpotential difference of −20 mV, suggesting the formation of a finer and more uniform zinc plating layer.

Another critical function of the additives into the electrolyte is to protect the zinc anode from corrosion during standby time of AZIBs. To elucidate the anticorrosion function, the LSV and EIS measurements were performed in the three-electrode cell configuration. Fig. 3b displays Polarization curves of zinc metal in $ZnSO_4$ 1M without and with 5 mM additives. As seen, there is almost no change in shape of the Tafel curves in terms of both cathode and anode branches. Only the electrolyte with 5 mM urea additive shows a bit shift in corrosion potential (∼10 mV) towards a negative potential direction compared with the electrolyte without the additive. The shift is less than 80 mV, implying mixed inhibition [23]. For further clarification, the polarization curves were analyzed by using Nova 2.1 software, the obtained results are listed in Table 1. Wherein, $E_{cor.}$, $i_{cor.}$ and H_i are corrosion potential, corrosion current density and inhibition efficiency, respectively.

It is apparent that the corrosion potential of the zinc metal almost remained after inclusion of the additives in the blank electrolyte. The corrosion potential was found to be around -1.01 V vs. SCE, suggesting the high activity of zinc metal in term of thermodynamic aspect. In general, the additives present in the electrolyte all show the protection ability of zinc metal from the corrosion of the electrolytes. The inhibition efficiency of the additives varied from 5.03% to 67.70%. This is attributed to the formation of the protective film on the zinc/electrolyte interface. Accordingly, the zinc anode in AZIBs was protected from the attack of corrosion agents such as H^+ and

dissolved O_2 in the electrolyte. The Tafel analysis results are in high agreement with the results from Fig. 1, which is related to the increase in the pH environment of the electrolyte after inclusion of the additives. Unfortunately, the results obtained from the EIS measurements (Fig. 3c) are hardly consistent with the results from the pH and LP measurements. From Fig. 3c, it is observed that the Nyquist plots of the electrolytes show a similar shape including a depressed semicircle. Thus, an equivalent circuit (inset in Fig. 3b) was proposed. Wherein, R_s represents solution resistance, R_{ct} is charge transfer resistance, and CPE is constant phase element, which represents surface heterogeneity caused by surface roughness, distribution of active sites, dislocation, or adsorption of the inhibitor molecules. Surprisingly, the magnitude (diameter) of the semicircle reduced after including the additive into the blank electrolyte. This indicates that the charge transfer resistance R_{ct} of zinc metal diminished in the presence of the additive in the electrolyte. In other words, based on EIS analysis data at OCP it can be inferred that the presence of additives in the electrolyte induced degraded anti-corrosion behavior of zinc. In fact, to investigate in detail other corrosion test methods should be applied.

To interpret further the effect of the additives on the zinc deposition process, which corresponds to the charge process of the zinc anode in AZIBs, the images of the zinc plating layer in the Hull cell containing the various electrolytes were captured and are displayed in Fig. 3d and Fig. 3e. The plating process was carried out at a current of 2 A for 5 min. Based on photographs of electrodeposits from Hull cell experiment, the optimum range of plating current density (denoted as $i_{opt.}$) for achieving the smooth zinc layer without dendritic growth was determined and enumerated in Table 1. The Figures indicate that, for the blank electrolyte, this range was from 3.9 to 10.2 A·dm^{-2}. In the presence of the additives in the electrolyte, the optimum range of plating current density varied slightly. Among them, it is worth noting that inclusion of the tyrosine additive narrowed the successful zinc deposition range. At the current densities less than 1.36 A·dm^{-2}, no zinc electrodeposition occurred. This implies that tyrosine hampered zinc deposition, which is consistent with the result obtained from CV measurements. On the contrary, in the presence of tryptophan the zinc plating layer was formed over the copper panel although at the low current density of 0.2 A·dm^{-2} the deposit was quite patchy (Fig. 3d). Besides, the cross-section image of the zinc plated - copper cathode in the Hull cell was captured and presented in Fig. 3e. Among the five tested additives, only urea, thiourea and tyrosine demonstrated ability of dendrite suppression with the rather flat surface while the other additives showed the apparent image of the blistered zinc plating layer or zinc dendrites formed at the edge of the copper panel.

To visually confirm the formation of zinc dendrites during AZIBs operation, a transparent symmetric cell was used. As shown in Fig. 4, at the current of 1 A after polarization for 2 min, zinc dendrites appeared in the cell. Obviously, adding serine and tryptophan in the electrolyte significantly promoted the zinc dendrites growth. The long dendrites freely grew toward the counter electrode. Meanwhile, the cell with urea, thiourea and tyrosine no zinc dendrite was observed. This is evidence for the benefit of urea, thiourea, and tyrosine in inhibition of the zinc dendrites growth. This result is in high agreement with the result obtained in Fig. 3e.

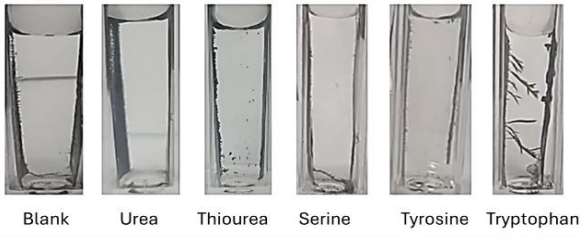

Fig. 4. Photographs of the transparent symmetric Zn/Zn cell with the electrolyte with and without 5 mM additives (urea, thiourea, serine, tyrosine and tryptophan) after polarization at 1 A for 2 min

3.2. Effect of the Additive Concentration

To determine the effect of the concentration of the additives on the formation of zinc dendrites, the dynamic morphology change of the metal zinc electrodes was recorded. As a typical sample, Fig. 5 and Fig. 6 show the zinc plating behavior in the electrolyte without and with urea and thiourea additives at the various concentrations from 5 mM to 100 mM. In general, at such a high volumetric current density of 333.3 A·dm^{-3} the surfaces of the zinc electrodeposition layers obtained in the electrolyte containing the urea and thiourea additives were found to be even and flat for the first minute of electrodeposition. However, when the electrodeposition time was prolonged, the zinc dendrites appeared. The growth of the zinc dendrites occurred dramatically when the additive concentration increased. As for the urea additive, after 5 min of electrodeposition, the formation of zinc dendrites was recorded in all the electrolytes including the electrolyte containing the low concentration of 5 mM urea. As for the thiourea additive, as shown in Fig. 6 it is surprising that, apart from the electrolyte containing 5 mM thiourea, when the concentration of thiourea increased from 10 mM to 100 mM, the dense density and increasing length of zinc dendrites electrodeposited on the zinc surface were recorded. This demonstrates that the thiourea impossibly suppresses zinc dendrites at high concentrations larger than 5 mM.

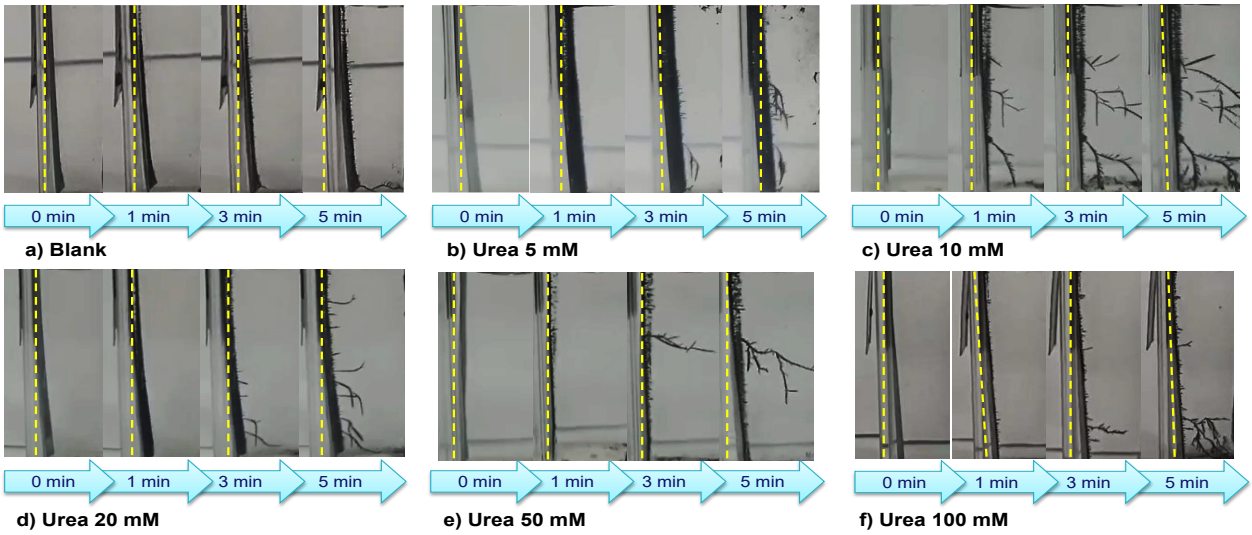

Fig. 5ne. In-situ optical images of initiation and growth process of zinc dendrites in the electrolyte (a) without and with urea additive at the different concentrations, (b) 5 mM, (c) 10 mM, (d) 20 mM, (e) 50 mM, and (f) 100 mM at a current of 1A

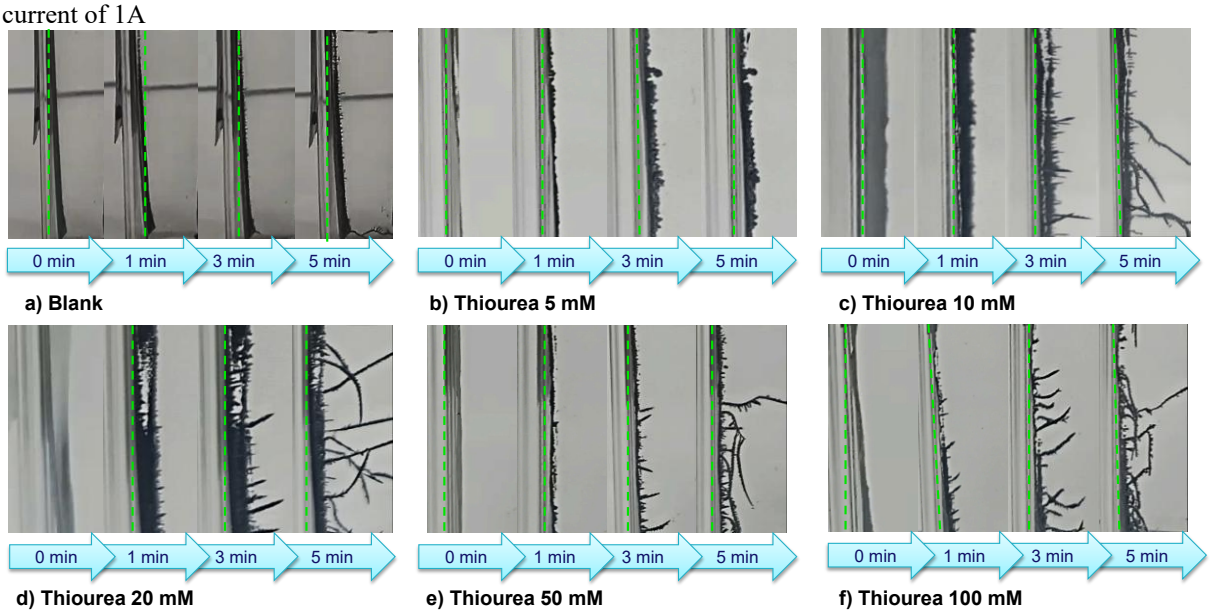

Fig. 6. In-situ optical images of initiation and growth process of zinc dendrites in the electrolyte (a) without and with thiourea additive at the different concentrations (b) 5 mM, (c) 10 mM, (d) 20 mM, (e) 50 mM, and (f) 100 mM at a current of 1A

4. Conclusion

This study investigated the effects of urea, thiourea, serine, tyrosine, and tryptophan as electrolyte additives for aqueous Zn-ion batteries. The results show that addition of the additives in the blank electrolyte hardly impacted significantly on the wettability and pH of the electrolyte. The hydrophilicity of zinc metal remained, which was manifested by the contact angle smaller than 90°, after inclusion of the additives in the electrolyte. The addition of urea, thiourea, and tyrosine was beneficial when their concentration was not over 5 mM. Increasing pH of urea, thiourea, and tyrosine to a neutral range partly contributed to improving interfacial resistance, reducing corrosion current density, and suppressing dendrite growth. By contrast, serine and tryptophan were ineffective and, even promoted dendrites. These findings indicate the potential of optimized organic additives to extend the cycle life and safety of AZIBs. However, to confirm positive effect of these additives the intensive investigations are indispensable. These investigated results will be reported in our subsequent publications in the near future.

Reference

[1] N. Gupta, N. Kaur, S. K. Jain, K. Singh Joshal, Chapter 3 - Smart grid power system, in Advances in Smart Grid Power System, A. Tomar and R. Kandari edited, Academic Press, 2021, pp. 47–71. https://doi.org/10.1016/B978-0-12-824337-4.00003-5

[2] S. Xu, J. Huang, G. Wang, Y. Dou, D. Yuan, L. Lin, K. Qin, K. Wu, H. K. Liu, S-X. Dou, and C. Wu, Electrolyte and additive engineering for Zn anode interfacial regulation in aqueous zinc batteries, Small Methods, vol. 8, iss. 6, Jun. 2024, Art. no. 2300268. https://doi.org/10.1002/smtd.202300268

[3] J. Yin, Y. Luo, M. Li, M. Wu, K. Guo, and Z. Wen, Electrolyte additive l-Lysine stabilizes the zinc electrode in aqueous zinc batteries for long cycling performance, ACS Applied Materials & Interfaces, vol. 16, iss. 39, Sep. 2024, pp. 53242–53251. https://doi.org/10.1021/acsami.4c11404

[4] Y. Zhang, X. Zheng, N. Wang, W.-H. Lai, Y. Liu, S.-L. Chou, H.-K. Liu, S.-X. Dou, and Y.-X. Wang, Anode optimization strategies for aqueous zinc-ion batteries, Chemical Science, vol. 13, no. 48, Oct. 2022, pp. 14246–14263. https://doi.org/10.1039/D2SC04945G

[5] W. Sun, F. Wang, S. Hou, C. Yang, X. Fan, Z. Ma, T. Gao, F. Han, R. Hu, M. Zhu, and C. Wang, Zn/MnO_2 battery chemistry with H^+ and Zn^{2+} coinsertion, Journal of the American Chemical Society, vol. 139, iss. 29, Jun. 2017, pp. 9775–9778. https://doi.org/10.1021/jacs.7b04471

[6] J. Tan, J. Liu, Electrolyte engineering toward high-voltage aqueous energy storage devices, Energy & Environmental Materials, vol. 4, iss. 3, Jul. 2021, pp. 302–306. https://doi.org/10.1002/eem2.12125

[7] M. H. Alfaruqi, V. Mathew, J. Gim, S. Kim, J. Song, J. P. Baboo, S. H. Choi, J. Kim, Electrochemically induced structural transformation in a γ-MnO_2 cathode of a high capacity zinc-ion battery system, Chemistry of Materials, vol. 27, iss. 10, May 2015, pp. 3609–3620. https://doi.org/10.1021/cm504717p

[8] H. Pan, Y. Shao, P. Yan, Y. Cheng, K. S. Han, Z. Nie, C. Wang, J. Yang, X. Li, P. Bhattacharya,K. T. Mueller, and J. Liu, Reversible aqueous zinc/manganese oxide energy storage from conversion reactions, Nature Energy, vol. 1, Apr. 2016, Art. no.16039 . https://doi.org/10.1038/nenergy.2016.39

[9] J. Hao, B. Li, X. Li, X. Zeng, S. Zhang, F. Yang, S. Liu, D. Li, C. Wu, and Z. Guo, An in-depth study of Zn metal surface chemistry for advanced aqueous Zn-Ion batteries, Advanced Materials, vol. 32, iss. 34, Aug. 2020, Art. no. 2003021. https://doi.org/10.1002/adma.202003021

[10] Z. Qi, T. Xiong, Z.G. Yu, F. Meng, B. Chen, H. Xiao, J. Xue, Suppressing zinc dendrite growth in aqueous battery via Zn–Al alloying with spatially confined zinc reservoirs, Journal of Power Sources, vol. 558, Feb. 2023, Art. no. 232628. https://doi.org/10.1016/j.jpowsour.2023.232628

[11] M. Wang, Y. Meng, X. Li, J. Qi, A. Li, and S. Huang, Challenges and strategies for zinc anodes in aqueous Zinc-Ion batteries, Chemical Engineering Journal, vol. 507, Mar. 2025, Art. no. 160615. https://doi.org/10.1016/j.cej.2025.160615

[12] F. Wang, O. Borodin, T. Gao, X. Fan, W. Sun, F. Han, A. Faraone, J. A. Dura, K. Xu, C. Wang, Highly reversible zinc metal anode for aqueous batteries, Nature Materials, vol. 17, Apr. 2018, pp. 543–549. https://doi.org/10.1038/s41563-018-0063-z

[13] X. Lv, X. Gu, R. Tian, H. Pan, X. Chen, J. Yang, D. Liu, and M. Wu, Artificial solid electrolyte interphases stabilized Zn metal anodes for high-rate and long-lifespan aqueous batteries, Electrochimica Acta, vol. 524, Jun. 2025, Art. no. 146053. https://doi.org/10.1016/j.electacta.2025.146053

[14] J. Chen, Y. Wang, Z. Tian, J. Zhao, Y. Ma, H. N. Alshareef, Recent developments in three-dimensional Zn metal anodes for battery applications, InfoMat, vol. 6, iss. 1, Jan. 2024, e12485. https://doi.org/10.1002/inf2.12485

[15] X. Zhu, W. Zhang, Z. Peng, L. Pan, B. Li, Z. Zhang, J. Zhu, W. Meng, L. Dai, L. Wang, and Z. He, Zinc-tin binary alloy interphase for zinc metal batteries, Chemical Engineering Journal, vol. 499, Nov. 2024, Art. no. 156521. https://doi.org/10.1016/j.cej.2024.156521

[16] L. Deng, X. Xie, W. Song, A. Pan, G. Cao, S. Liang, and G. Fang, Realizing highly stable zinc anode via an electrolyte additive shield layer and electrochemical in-situ interface, Chemical Engineering Journal, vol. 488, May. 2024, Art. no. 151104. https://doi.org/10.1016/j.cej.2024.151104

[17] J. Cao, F. Zhao, W. Guan, X. Yang, Q. Zhao, L. Gao, X. Ren, G. Wu, A. Liu, Additives for aqueous Zinc-Ion batteries: recent progress, mechanism analysis, and future perspectives, Small, vol. 20, iss. 33, Aug. 2024, Art. no. 2400221. https://doi.org/10.1002/smll.202400221

[18] T. Liu, X. Dong, B. Tang, R. Zhao, J. Xu, H. Li, S. Gao, Y. Fang, D. Chao, Z. Zhou, Engineering electrolyte additives for stable zinc-based aqueous batteries: insights and prospects, Journal of Energy Chemistry, vol. 98, Nov. 2024, pp. 311–326. https://doi.org/10.1016/j.jechem.2024.06.036

[19] S. A. Haris, S. Adhami, R. Yuksel, and S. O. Kim, Bio-inspired Zinc anodes: mitigating dendrite formation and side reactions in aqueous Zinc metal batteries using laser carbonized chitosan layer, Nano and Micro Small, vol. 21, iss. 18, May 2025, Art. no. 2501293. https://doi.org/10.1002/smll.202501293

[20] S. Lee, S.-H. Huh, Y.-H. Lee, S. H. Kim, J.-S. Bae, K. -S. Ahn, J. Huh, Y. -E. Sung, and S.-H. Yu, Exploring the effects of biomolecular additive on performance of aqueous zinc metal batteries, Chemical Engineering Journal, vol. 515, Jul. 2025, Art. no. 163465. https://doi.org/10.1016/j.cej.2025.163465

[21] Y. Guo, R. Zhao, Z. Xu, C. Q. Lai, Enhancing Zn anode stability with bioderived electrolyte additive for aqueous

Zn-ion batteries, Journal of Power Sources, vol. 643, Jul. 2025, Art. no. 237071. https://doi.org/10.1016/j.jpowsour.2025.237071

[22] G. Jiang, L. Guo, M. Shao, N. Liu, Z. Bai, N. Wang, H. Peng, and X. Jiang, Bio-derived chitosan additive enables anion anchoring and Zn(002) deposition for high-performance Zn anodes, Chemical Communications, vol. 61, Apr. 2025, pp. 7612–7615. https://doi.org/10.1039/D5CC01325A

[23] H. T. Bui, T.-D. Dang, H. T. Le, and T. T. Hoang, Comparative study on corrosion inhibition of vietnam orange peel essential oil with urotropine and insight of corrosion inhibition mechanism for mild steel in hydrochloric solution, Journal of Electrochemical Science and Technology**,** vol. 10, iss. 1, Mar. 2019, pp. 69–81. https://doi.org/10.5229/JECST.2019.10.1.69

[24] G. Nikiforidis, R. Cartwright, D. Hodgson, D. Hall, L. Berlouis, Factors affecting the performance of the Zn-Ce redox flow battery, Electrochimica Acta, vol. 140, Sep. 2014, pp. 139-144. https://doi.org/10.1016/j.electacta.2014.04.150

[25] R. T. Vashi, K. Desai, Aniline as corrosion inhibitor for zinc in hydrochloric acid, Chemical Science Transactions, vol. 2, no. 2, 2013, pp. 670–676.

[26] Y. Zhao, C. Cao, N. Zhang, F. Liang, H. Dong, H. He, S. Li, Y. Feng, R. Li, W. Gu, B. Fei, and M. Ge, Multifunctional electrolyte additives enabled adaptable interface toward stabilizing Zn metal anodes, Chemical Engineering Journal, vol. 504, Jan. 2025, Art. no. 158737. https://doi.org/10.1016/j.cej.2024.158737

[27] X. Yan, Y. Tong, Y. Liu, X. Li, Z. Qin, Z. Wu, and W. Hu, Highly reversible Zn anodes through a hydrophobic interface formed by electrolyte additive, Nanomaterials, vol. 13, iss. 9, 2023. https://doi.org/10.3390/nano13091547

[28] Z. Peng, S. Li, L. Tang, J. Zheng, L. Tan, and Y. Chen, Water-shielding electric double layer and stable interphase engineering for durable aqueous zinc-ion batteries, Nature Communications, vol. 16, 2025, Art. no. 4490. https://doi.org/10.1038/s41467-025-59830-y